JOURNAL OF MATERIALS SCIENCE 8 (1973) 777–786

The temperature dependence of microhardness of the transition-metal carbides

D. L. KOHLSTEDT*
Surface Physics, Cavendish Laboratory, University of Cambridge, UK

Microhardness as a function of temperature has been measured for single crystals of $TiC_{0.96}$, $ZrC_{0.94}$, and $NbC_{0.87}$ from room temperature through their ductile-brittle transitions and for single crystals of V_6C_5 through the order-disorder transition. The present data confirm the result observed for polycrystalline specimens that for $T < 0.5\ T_m$, the decrease in hardness with increasing temperature for the carbides is substantially more rapid than for metals and semiconductors. Above the ductile-brittle transitions, the ratios of hardness to yield stress are factors of 1.5 to 3 larger than calculated from theory. We suggest that the larger values result from the higher strain-rates and larger strains involved in the hardness tests. Arrhenius plots of the hardness data for $T > 0.25\ T_m$ are linear and exhibit changes in slope near 0.33 and 0.44 T_m. The former temperature is near the ductile-brittle transition temperature for the disordered carbides, and the latter is at the temperature for which a similar change in Arrhenius slope occurs in published yield-stress data. In addition, a change in slope is found for VC at 0.48 T_m (1275 °C) which is the order-disorder transition temperature for $V_6C_5 \rightarrow VC_{0.84}$. These changes in slope are suggestive of corresponding changes in the thermally-activated processes governing plastic flow.

1. Introduction

Characteristic of the carbides of the group IV and group V transition metals is a phase with the familiar NaCl structure. The carbon sublattice in this phase can support from 1 to 50% vacant sites [1] and, with the exception of V_6C_5 [2], exhibits no long-range ordering. The most outstanding physical properties of the cubic transition-metal carbides are their extreme strengths and high melting temperatures.

To study the plastic flow of a carbide from room temperature to near its melting point (~3000 to 4000°C), two distinctly different techniques are required. In the brittle region (below one-third a cubic carbide's melting temperature), microhardness indenting is used because the large hydrostatic pressure under the indenter prevents brittle failure [4, 5]. In the ductile region, uniaxial loading or bending methods are necessary because the sharp edges of the indenter blunt either by softening or chemical reaction. The latter technique is preferable because during hardness indenting neither the stress nor the strain-rate is homogeneous [6], and the latter can be orders-of-magnitude larger than in uniaxial measurements. Yet, the hardness test remains a valuable technique, for it provides, at the very least, a relative measure of yield strengths of solids that are otherwise brittle.

Both the hardness and the yield stress as functions of temperature have been studied for the disordered carbides. Hardness data [9-12], which are available for polycrystalline specimens well into the ductile region, demonstrate that the yield strength of the carbides decreases nearly ten times more rapidly with increasing temperature than does the hardness of other covalent solids such as Si and Ge [9]. Yield stress, which also falls rapidly, decreases exponentially with increasing temperature [3, 13, 14]. An Arrhenius plot of yield stress data is characterized by more

*Present address: Department of Earth and Planetary Sciences, Massachusetts Institute of Technology, Cambridge, Massachusetts 02139, USA.

than one linear region, suggesting that at least two thermally activated processes may be important in plastic flow of the carbides [3]. Williams [3] has pointed out that an extrapolation of yield-stress data to room temperature gives a value several orders-of-magnitude higher that estimated from hardness data. He suggests, therefore, that if thermally activated mechanisms are involved, at least one more process with a lower activation energy is required to connect the high- and low-temperature results. Previous hardness studies have not examined this point.

In the ordered carbide V_6C_5, the ductile-brittle transition is coincident with the order-disorder transition near $T_m/2$. As found for the disordered carbides, the yield stress of $VC_{0.84}$ above the ductile-brittle transition temperature is an exponential function of inverse temperature [13]. Room-temperature hardness measurements on V_6C_5 have demonstrated that anti-phase domain boundaries (APB's) impede disolocation motion [15]. However, no one has provided data connecting the low-temperature and high-temperature results and demonstrating a change in mechanical strength associated with the disordering of the carbon sublattice and the removal of the domain boundaries.

The present paper reports the hardness of single crystals of TiC, ZrC, VC, and NbC from room temperature to above the ductile-brittle transition as measured from micro-indentations. These data are compared with earlier hardness results on polycrystalline specimens, and correlation is made with yield-stress data. The Arrhenius nature of the hardness results is examined (a) above the ductile-brittle transition to determine whether the two linear regions observed in yield-stress measurements can be detected in hardness studies, and (b) below the transition to test for the existence of an additional thermally activated mechanism. Finally, for V_6C_5 particular attention is given to the effect of the order-disorder transition on hardness.

2. Experimental

The specimens indented were as-grown, single crystals with the following carbon-to-metal ratios: $TiC_{0.96}$, $ZrC_{0.94}$, $VC_{0.84}$, and $NbC_{0.87}$. The ZrC, VC, and NbC crystals were grown by the floating-zone technique [16], and their carbon-to-metal ratios were determined by chemical analysis. The TiC crystal was grown by the Linde Division of Union Carbide Corporation by the arc-Verneuil process [17], and its carbon-to-metal ratio was found by comparison of its room-temperature Vickers hardness with Williams' data on TiC for Vickers hardness versus carbon-to-metal ratio [18]. The major impurities of the crystals were oxygen and nitrogen, which were present at levels of less than 0.01 wt %.

With the crystals oriented to the (001) by Laue back-reflection, discs of 1 cm diameter and 0.5 mm thickness were sliced with a spark eroder. The discs were metallographically polished to a 3 μm diamond finish, then etched in a ceric oxide-sulphuric acid slurry to remove the worked layer [19], which, in the case of V_6C_5, made visible its optical domain structure when viewed through crossed polarizers [2]. The V_6C_5 specimens had optical domains averaging 5 μm across, corresponding to a cooling rate through the order-disorder transition of 10°C sec^{-1} [15].

Indentation experiments were carried out in a vacuum of 5×10^{-5} to 1×10^{-4} Torr in the high-temperature indenting apparatus described in a separate paper [20] with a load of 500 g [15]. The load was lowered at a rate of 10 μm sec^{-1}, approximately one-third that of a commercial Leitz mini-load hardness tester, and applied for 10 sec. Both Knoop and Vickers indenters were used. At least five indentations were made at each temperature, and all indentations for a given run were made with parallel diagonals to eliminate variations in hardness due to hardness anisotropy which can be as large as 25% in the carbides [18, 21]. However, the crystallographic direction of the indenter diagonal was arbitrary and, except for ZrC, was varied from one run to the next. The length of each indentation was measured twice in a metallurgical microscope at a magnification of either × 200 or × 500.

Three specimens each of TiC, ZrC, VC, and NbC were indented with a Knoop diamond indenter from room temperature to approximately 1000°C. Because of the failure of the indenter tips by graphitization in the case of diamond and fracture in the case of B_4C, an assortment of indenters was used above 1000°C. One VC specimen was successfully indented from room temperature to 1500°C with a Knoop diamond indenter as well as at 1300, 1400, and 1500°C with a Vickers, B_4C indenter; data for one ZrC specimen were obtained from room temperature to 1130°C with a second Knoop diamond indenter; and acceptable indentations

were made in one specimen of NbC from 1000 to 1510° C with a Knoop B_4C indenter.

To reveal the dislocation distribution near the indentations, TiC and ZrC specimens were etched in boiling H_2SO_4 [17] and VC and NbC were etched in a warm 40 HCl: 10 HNO_3: 1 HF bath for several minutes [22].

3. Results

Representative hardness versus homologous temperature data for TiC, ZrC, VC, and NbC are presented in Fig. 1, and ln hardness versus inverse temperature data are plotted for these four carbides in Figs. 2 to 5, respectively. The slopes and associated homologous temperature regions of the Arrhenius plots are given in Table I; the values used for T_m are the liquidus temperatures [35]. In Figs. 3 and 5, the error bars indicate the estimated error in the hardness when it is greater than 4%. Indentations yielding hardness values with uncertainties of less than 4% were made with indenters that had sharp, flawless edges and point, and the uncertainties were taken as the standard deviation of the five or more indentations made at a single temperature. Errors in the slopes associated with these data are less than 6%. Errors of greater than 4% were encountered when the indenter edge or tip deteriorated during a run, either by fracturing, as for B_4C, or by graphitization, as for diamond, and were estimated at 20% by comparing "perfect" and "imperfect" indentations made at the same temperature. If more than 5% of an indentation was affected by the damaged

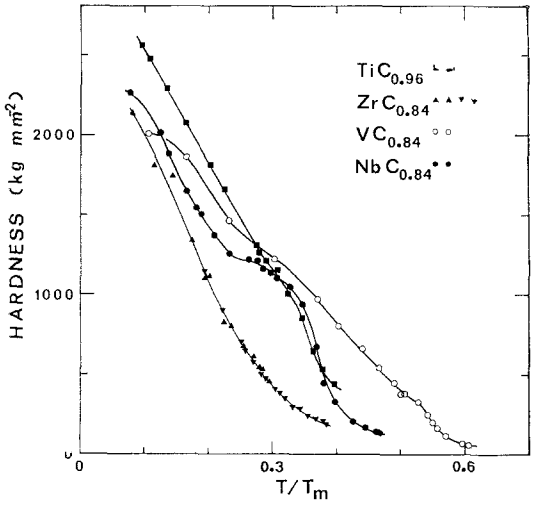

Figure 1 Hardness versus homologous temperature for TiC, ZrC, VC, and NbC.

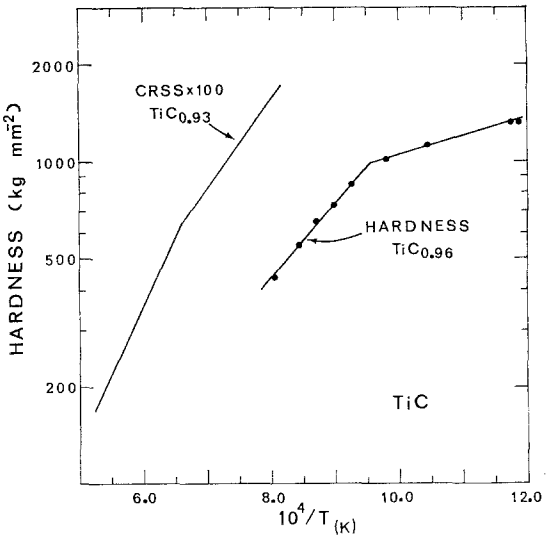

Figure 2 Log hardness versus inverse temperature for TiC. CRSS results are presented for comparison [3].

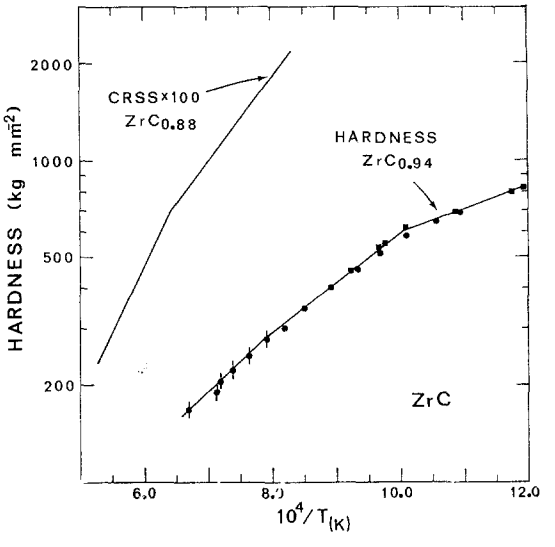

Figure 3 Log hardness versus inverse temperature for ZrC. CRSS results are presented for comparison [3].

portion of the indenter, the data point was rejected. The uncertainty in the slopes of the straight lines fitted to these less certain data is approximately 30%. The straight lines through the data points represent best fits, assuming a regionally linear relation between ln hardness and inverse temperature.

For TiC, Fig. 2, the data from only one run are presented; the results of all three runs are in good agreement, as evidenced by a standard deviation of 10% in their slopes. Because the crystallographic orientation of the indenter

TABLE I Arrhenius slopes of present hardness results from Figs. 2 to 5. The slopes are calculated from $\partial(\ln H)/\partial(1/T)$.

Carbide	T_m (°C)	Temperature range (T/T_m)	Slope (10^4K)
$TiC_{0.96}$	3025	~0.25 to 0.32	0.14
		0.32 to 0.38	0.53
$ZrC_{0.94}$	3400	~0.25 to 0.34	0.34
		0.34 to 0.41	0.4 (5)
$VC_{0.84}$	2950	~0.25 to 0.32	0.04
		0.32 to 0.42	0.27
		0.42 to 0.48	0.66
		0.48 to 0.55	2.14
$NbC_{0.87}$	3600	~0.25 to 0.34	0.09
		0.34 to 0.45	0.9
		0.45 to 0.48	1.1

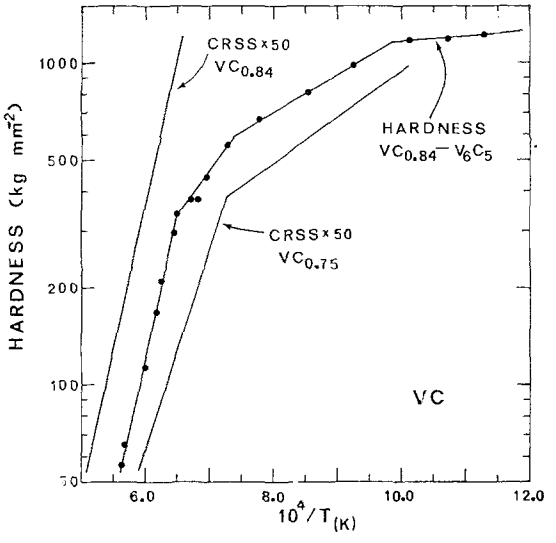

Figure 4 Log hardness versus inverse temperature for VC. CRSS results are presented for comparison [13].

diagonal differed for each of the three runs, the Arrhenius plot of hardness for one run was nearly parallel, though not colinear, with that of the next. As is done for the other carbides discussed below, the published results for critical resolved shear stress (CRSS) are also sketched for comparison.

The hardness of ZrC versus inverse temperature for two series of indentations with parallel diagonals, one from room temperature to 800°C and one from room temperature to 1130°C, are plotted in Fig. 3 to demonstrate the reproducibility obtainable with our apparatus. As with TiC, the slopes for the other two runs to 800°C agree well with those calculated from the data in Fig. 3.

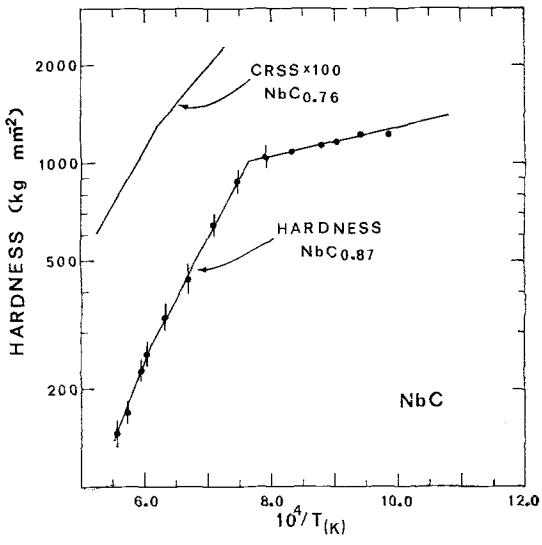

Figure 5 Log hardness versus inverse temperature for NbC. CRSS results are presented for comparison [3].

Slopes calculated from the data for the room temperature to 1500°C run on VC, Fig. 4, are in good agreement (10%) with those of the three runs to 1000°C in the region of overlap. The diamond indenter used for the 1500°C run, and previously for TiC, NbC, and VC to 1000°C, began to graphitize at 1500°C. The hardnesses obtained at 1300, 1400, and 1500°C with the B_4C Vickers indenter agree within 10% with the data of Fig. 4.

Two sets of data are shown for NbC in Fig. 5; one is representative of the three runs made with the Knoop diamond from room temperature to 930°C and the other is the data obtained with a slightly damaged B_4C Knoop indenter from 1000 to 1510°C.

The most outstanding feature of the Arrhenius plots of hardness is the distinct linear regions into which the data fall. It is difficult to imagine that a smooth curve would be more appropriate for any of the data, except possibly that of ZrC, and the precedent set by the data for TiC, VC, and NbC provides ample justification for fitting straight lines to the ZrC results also.

4. Discussion

4.1 Previous hardness-temperature data

As early as 1955, Westbrook [7] studied the hardness of TiC from room temperature to 700°C. More recently, several additional investigations of hardness versus temperature have

been reported for the carbides [8-12]; the temperature range and references for these investigations are collated in Table II. For comparison, the data for TiC of these authors are plotted with those of the present study in Fig. 6.

The agreement among the six sets of data presented in Fig. 6 is thought to be quite good considering the fact that several details differ from one experimenter to the next. Only the present study and that of Atkins and Tabor [9] use single-crystal specimens, but the two studies differ in that above 600°C the latter employed mutual-indentation techniques while the former involves only the micro-indentation method. In those experiments involving sintered carbides, density and grain-size are important factors which could account for deviations among the several authors' results. Another parameter influencing the hardness of the carbides is stoichiometry; for example, at room temperature $TiC_{0.94}$ is 140% harder than $TiC_{0.73}$ and this discrepancy is increased at 1000°C to 180% [12]. Certainly impurities, particularly oxygen and nitrogen which readily occupy vacant carbon sites in the lattice, also influence the hardness.

In addition to the properties of the specimens, the nature of the indentation process is important. Firstly, parameters such as the rate of loading and time of application of the load are important; the former controls the strain-rate, and the latter, especially at high temperatures, effects the distance the indenter penetrates the specimen and thus the indentation size and corresponding hardness [6]. Secondly, both micro- and mutual-indentation techniques, which differ substantially in detail, were used. Finally, both Knoop and Vickers micro-indentations are sensitive to crystallographic orientation of the indenter diagonal, varying 25 and 10% respectively, between the [100] and [110] on the (001) for TiC [21].

TABLE II Previous hardness studies on transition-metal carbides.

Carbides	Temperature range	Reference
TiC	25 to 700°C	Westbrook [7]
TiC and NbC	25 to 1200	Miyoshi and Hara [8]
Tic	25 to 1900	Atkins and Tabor [9]
TiC and NbC	1000 to 1600 and 1000 to 1800	Koester and Moak [10]
Tic, ZrC, VC, NbC	−25 to 900	Westbrook and Stover [11]
Tic	25 to 2000	Samsonov *et al* [12]

Although agreement within the carbide family for the several investigations is fairly good (Figs. 1 and 6), a comparison in Fig. 7 of hardness versus temperature below $T_m/2$ for TiC with that for Cu, Ge, and Si [9] reveals an enormously rapid decrease in hardness with increasing temperature for TiC. A search for an explanation of this large rate-of-change in hardness with temperature has recently been presented as part of an investigation of the influence of temperature on the active slip systems in the carbides [21].

Hannink *et al* [21] have shown, by measuring the anisotropy in hardness (i.e., the dependence of hardness on the orientation of the long axis of a Knoop indenter) and by employing the analysis of Brookes *et al* [23], that the active slip system in TiC undergoes a change near 200°C. In their analysis of the resolved shear stresses under an indenter on the active, crystallographic slip systems, Brookes *et al* formulated an equation which relates the effective resolved shear stress to hardness anisotropy and correctly predicts the active slip systems of more than twenty crystals of six different crystal structures. Application of this analysis to hardness-anisotropy data at several temperatures for TiC, shows that in the low temperature regime ($T \lesssim 200$°C) the $\{110\}\langle 1\bar{1}0\rangle$ system is active, in the intermediate regime ($200 \lesssim T \lesssim 600$°C) both the $\{110\}\langle 1\bar{1}0\rangle$ and the $\{111\}\langle 1\bar{1}0\rangle$ systems are active, and in the high temperature regime ($T \lesssim 600$°C) the $\{111\}\langle 1\bar{1}0\rangle$ system is active. These three temperature regimes also exist, though at different temperatures, for the other cubic, transition-metal carbides.

The change from the $\{110\}\langle 1\bar{1}0\rangle$ to the $\{111\}\langle 1\bar{1}0\rangle$ slip system with increasing temperature and the rapid drop in hardness with increasing temperature suggest that covalent bonding between carbon and metal atoms, thought to be important in the carbides [24], is reduced in strength with increasing temperature. We suggest that at lower temperatures the high directionality of the covalent bonds inhibit slip on the close-packed $\{111\}$ planes, and that the strength of these bonds results in low dislocation mobility and room-temperature brittleness; however, as the temperature is increased, high-mobility s electrons are thermally activated and

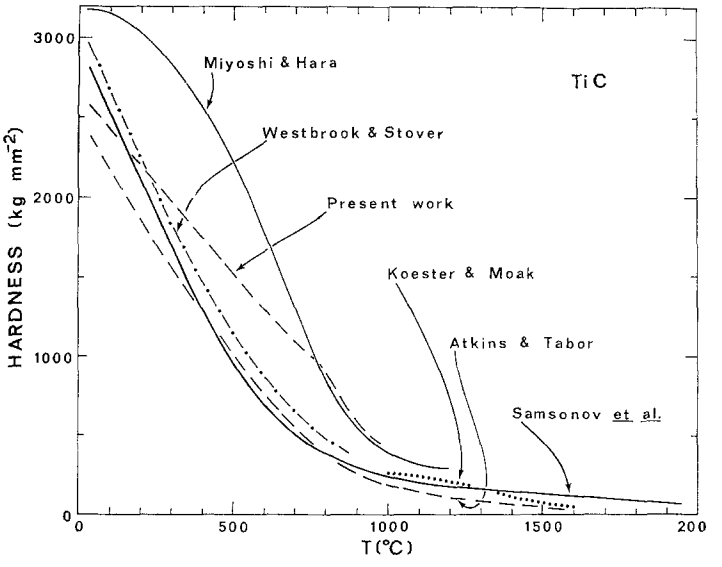

Figure 6 Summary of hardness versus temperature results for TiC [8-12].

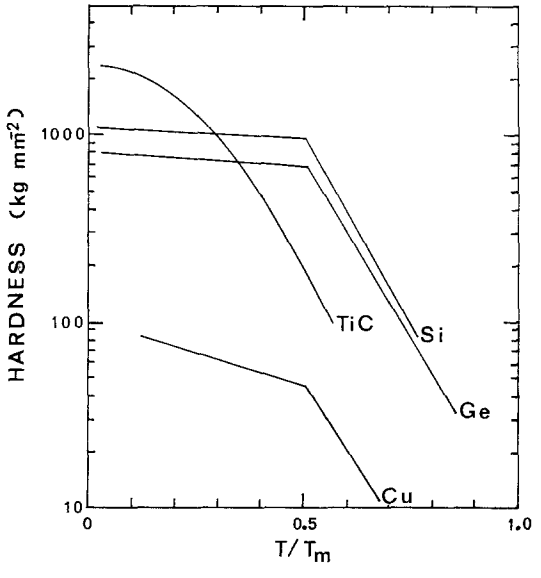

Figure 7 Log hardness versus homologous temperature for Si, Ge, Cu [6], and TiC [present work].

screen the hybridized orbitals which form the covalent bonds, thus affecting the rapid decrease from covalent-like hardness at low temperatures to metallic-like hardness at elevated temperatures by permitting slip to occur on the $\{111\}\langle 1\bar{1}0\rangle$ system [21]. The temperature-dependence of the Hall coefficient [25, 26] provides experimental evidence for an increase in the conduction electron population as the temperature increases, an effect especially marked for $TiC_{0.96}$.

4.2. Comparison with yield stress

Hill [4] and Tabor [5], using the condition that the hydrostatic pressure under the indenter plays no role in the plastic deformation, have analysed the indentation process to show that hardness, H, is related to yield stress, Y, by

$$H = 3Y;$$

that is, two-thirds of the pressure under the indenter is hydrostatic and one-third is shear stress; only the latter produces plastic flow. This equation is derived assuming that the indented solid is isotropic and fully work-hardened and that elastic deformation is unimportant. For many metals, this expression is well obeyed [6].

To extend the analysis to a broader range of solids, Marsh [27] considered the role of elasticity in the indentation process. He suggested that elastic deformation of the "hinterland" was important and used as a model hydrostatic pressure expanding a spherical cavity in a plastic-elastic solid. In 1950, Hill [4] showed that for a solid with Young's modulus E and Poisson's ratio ν

$$H = \frac{2}{3}\left[1 + \ln\frac{E}{3(1-\nu)\,Y}\right]Y.$$

Empirically, Marsh [27] found that

$$H \simeq 0.07 + 0.6\ln\frac{E}{Y}$$

and theoretically Johnson [28] showed that

$$H = \frac{2}{3}\left[\frac{1 + \ln E \cos\theta}{3Y}\right]Y$$

where θ is the semi-angle of the indenter. For the carbides at 1000°C, with Poisson ratio near 0.2, Young's modulus in the order of 3×10^4 kg mm^{-2} [29] and yield stress in the order of 30 kg mm^{-2} [3], all three equations for H yield

$$H \simeq 4.5Y.$$

A comparison of the present hardness results with the yield-stress or CRSS data of Williams [3] and Hollox [13], Figs. 2 to 5, demonstrate that H/Y has a value between 6 and 12, dependent on the carbide and temperature considered. The fact that the experimental ratio is larger than predicted suggests that the strain-rates involved in the hardness experiments are substantially higher than in the yield-stress studies. Williams [3] has shown that yield stress is a sensitive function of strain-rate for the carbides; for example, when the strain-rate for TiC at 1400°C is increased from 2×10^{-4} sec^{-1} to 2×10^{-2} sec^{-1}, the critical resolved shear stress increases from 3 to 10 kg mm^{-2}. This direction and magnitude of the change in yield stress with increased strain-rate indicates that in comparing hardness and yield-stress data account should be taken of strain-rate differences. The large experimental values of H/Y also partly result because the total strain involved in the uniaxial compression tests, 1% [3], is smaller than in hardness measurements, 8% [6].

It is not unusual for rocksalt-structured solids to exhibit a high hardness-to-yield stress ratio, $H/Y \simeq 30$ [30]. In ionic solids, high H/Y values are thought to reflect the fact that the deformation under the indenter is constrained because the $\{1\,1\,0\}\langle 1\bar{1}0\rangle$ slip system does not fulfill the von Mises criterion. In the present case, however, H/Y values are calculated in the temperature regime in which the $\{1\,1\,1\}\langle 1\,1\,0\rangle$ slip system is active in the carbides so that an arbitrary shape change can be accommodated. This feature of high-temperature deformation of the carbides, as contrasted with ionic crystals, has also been discussed in relation to the lack of cracking in deformed polycrystalline samples [18]. (At room temperature TiC slips on $\{1\,1\,0\}\langle 1\bar{1}0\rangle$ so that H/Y may approach a value of 30 at lower temperatures.)

4.3. Arrhenius nature

Two features stand out in the Arrhenius plots of the present hardness data, Figs. 2 to 5. Firstly, ln H and $1/T$ are linearly related and, secondly, several linear regions exist. Williams [3] observed these same features in his ln CRSS versus $1/T$ data for TiC, Fig. 2; and Figs. 3 and 5 indicate that his CRSS data for ZrC and NbC follow the same pattern.

Since Williams' observation, several investigations of deformation of the carbides have reported (a) in the case yield-stress or flow-stress measurements, the existence of more than one linear Arrhenius region [3, 13, 14, 31] or (b) in the case of creep studies, a change from one activation energy to a second with increasing temperature [18, 32-34]. These Arrhenius slopes and activation energies with associated homologous temperature ranges are presented with the mode of deformation and reference in Table III. Because Kelly and Rowcliffe [14] do not take a stress exponent into account in calculating their activation energies, the Arrhenius slopes which we calculated from their energies are tabulated. We also computed the slope values which are presented from the data of Williams [3] and of Hollox [13]. A recent hardness versus temperature study by Samsonov *et al* [12] is deleted because their analysis relies on "a rather unusual creep relation" [6].

The general conclusion to be drawn from Tables I and III is that transitions from one Arrhenius region or activation energy to the next occur at rather well-defined homologous temperatures for the carbides:

$$\begin{aligned}
&TR_1\text{: } (0.25)? \lesssim T < 0.33\,T_m\\
&TR_2\text{: } 0.33 \lesssim T < 0.46\,T_m\\
&TR_3\text{: } 0.46 \lesssim T < 0.66\,T_m\\
&TR_4\text{: } 0.66 \lesssim T < (?\ \ T_m)\ .
\end{aligned}$$

(Hardness data for ordered VC exhibit an additional change in slope at its order-disorder temperature.)

Although definite transitions occur near 0.33 T_m, 0.46 T_m, and 0.66 T_m, additional experimental evidence is necessary to confirm the lower bound of TR_1 and the upper bound of TR_4. It should be emphasized (a) that the transition near 0.46 T_m first found in CRSS data [3] and dislocation-loop annealing-rate data [35] are also observed in the present hardness results, and (b) that the transition near 0.33 T_m, first noted in the present work, is in the proximity

TABLE III Slopes or activation energies with associated temperature ranges from constant strain-rate ($\dot{\epsilon}$), constant stress (σ), and electron microscopy (EM) experiments for single crystals (S) and polycrystals (P). The slopes are calculated from $\partial(\ln H)/\partial(1/T)$.

Carbide	Form	Temperature range (T/T_m)	Slope (10^4K)	Activation energy (eV)	Techniques	Reference
$TiC_{0.97}$	S	0.36 to 0.46	—	2.3	$\dot{\epsilon}$	Hollox [13]
$TiC_{0.95}$	S	0.33 to 0.45	0.6	—	$\dot{\epsilon}$	Williams [3, 18]
		0.45 to 0.57	0.9	3		
$TiC_{0.97}$	P	~0.46	—	3	$\dot{\epsilon}$	Murray [31]
		0.46 to 0.61	—	6		
$TiC_{0.93}$	S	0.50 to 0.60	—	3.3	σ	Williams [18]
$TiC_{0.97}$	P	~0.58	—	5.6	σ	Keihn and Kebler [32]
		~0.63	—	7.6		
$TiC_{0.75}$	P	0.54 to 0.66	0.7	—	$\dot{\epsilon}$	Kelly and Rowcliffe [14]
		0.66 to 0.70	2.4	—		
$TiC_{0.96}$	S	<0.48	—	3.4	EM	Hollox and Smallman [35]
		>0.48	—	5.3		
$ZrC_{0.88}$	S	0.32 to 0.42	0.6	—	$\dot{\epsilon}$	Williams [3]
		0.42 to 0.51	0.9	—		
$ZrC_{0.98}$	P	0.56 to 0.66	—	3.3	σ	Leipold and Nielsen [33]
		0.66 to 0.76	—	8.7		
$ZrC_{0.98}$	S	0.46 to 0.67	—	4.8	σ	Lee and Haggerty [34]
$VC_{0.84}$	S	0.48 to 0.66	2.1	—	$\dot{\epsilon}$	Hollox [13]
$VC_{0.75}$	S	0.33 to 0.45	0.7	—	$\dot{\epsilon}$	Hollox [13]
		0.45 to 0.56	1.5	—		
$VC_{0.61}$	P	0.50 to 0.69	0.7	—	$\dot{\epsilon}$	Kelly and Rowcliffe [14]
		0.69 to 0.81	2.3	—		
$NbC_{0.76}$	S	0.34 to 0.42	0.5	—	$\dot{\epsilon}$	Williams [3]
		0.42 to 0.49	0.8	—		
$NbC_{0.95}$	P	0.48 to 0.61	0.6	—	$\dot{\epsilon}$	Kelly and Rowcliffe [14]
		0.61 to 0.64	2.2	—		

of the strain-rate sensitive [3], ductile-brittle transition temperature found in uniaxial compression measurements.

Two points relevant to the discussion of thermally activated mechanisms for plastic flow emerge from the present work. Firstly, not only above but also below the ductile-brittle transition temperature, hardness fits a linear Arrhenius plot and thus can be expressed as $H \propto \exp(Q/RT)$, where Q is the activation energy governing plastic flow. The change in slope of ln H versus $1/T$ near the ductile-brittle transition suggests a corresponding change in mechanism controlling the dislocation dynamics. Williams [3] noted the necessity for a new mechanism, so as to provide agreement, at room temperature, between extrapolated yield-stress results and hardness data. Secondly, above the ductile-brittle transition, at least three Arrhenius regions well defined in temperature, exist. One interesting correlation to be noted, though it may be fortuitous, is that the high-temperature transition occurs near 2/3 T_m, Shewmon's "rule-of-thumb" temperature [36] for the transition from a dominant mass transfer process of short-circuited diffusion to one of bulk diffusion. This observation may be important if deformation in TR_3 and TR_4 is governed by creep due to dislocation climb as is the case for metals above 0.5 T_m [37].

Ideally we would like to analyse our hardness data to obtain activation energies for each temperature region. Below $T_m/2$ no theory exists for extracting activation energies. However, it is interesting to note that the Arrhenius slopes from yield-stress and hardness data are in fair agreement, $\pm$ 30%, considering the inherent differences in the two techniques and the stoichiometry variations between carbide specimens.

Above $T_m/2$ (i.e. for temperatures sufficiently high so that diffusion is important), Atkins *et al* [38] have analysed the indentation process in terms of transient creep controlled by dislocation climb and found for a constant load application time

$$H = K_1 \exp(Q/m\,RT)$$

where K_1 is a constant and m is defined in the steady-state creep relation for strain rate $\dot{\epsilon}$ and stress σ

$$\dot{\epsilon} = K_2 \sigma^m \exp(-Q/RT) .$$

Tabor [6] has pointed out that the same equation for H results if steady-state, rather than transient creep, is assumed. The determination of the activation energy, then, depends upon the choice of m.

Creep experiments above 0.5 T_m have generally yielded values for m on the order of 5 [37]; $m = 5$ is also consistent with values found in the single crystal, steady-state creep studies on ZrC [34]. However, Atkins *et al* [38] found that for Al, Sn, and MgO $m \simeq 10$ is more appropriate for the high stresses ($\sigma > 10^{-3}$elastic modulus) involved in the indentation process.

Of the present hardness data, only that for VC extends to $T > T_m/2$. Activation energies calculated from these data are 9.3 eV for $m = 5$ and 18.6 for $m = 10$. The latter value for the activation energy appears to be much too large to be consistent with known energies for thermally activated processes in the carbides. The 9.3 eV value is in reasonable agreement with activation energies of 7.6 eV [32] and 8.7 eV [33] for high-temperature, steady-state creep in TiC and ZrC, respectively. These activation energies might be associated with metal diffusion which is known to proceed with an activation energy of 7.7 eV in TiC [39]. However, the uncertainties in calculating the 9.3 eV energy from the Arrhenius slope of the hardness data and the lack of diffusional data for V in VC make the identification of this energy tenuous at best.

The identification of mechanisms controlling plastic deformation in the carbides is a complex problem, requiring both more theory and more data than are presently available. Processes, such as surmounting a high Peierls barrier, dislocation interaction, debris formation, and diffusion, are all undoubtedly important. These various mechanisms have been discussed in the light of diffusion measurements [39-41] and electron-microscope observations [31, 34, 35] in recent reviews [13, 42, 43].

4.4. Order-disorder transition

The transition from V_6C_5 to $VC_{0.84}$ near 1275°C is marked by a distinct change in slope in both the hardness-temperature and the ln hardness-inverse temperature plots, Figs. 1 and 4. Consistent with the other carbides studied, the Arrhenius plot of hardness for VC also undergoes changes in slope near 0.33 T_m and 0.44 T_m. The similarity in the Arrhenius nature of VC and the other carbides suggests that the basic mechanisms that limit dislocation motion in the non-ordered carbides are important also for ordered VC. However, the less rapid decrease in hardness with increasing temperature below and the large change in Arrhenius slope at the transition temperature demonstrate that the ordering acts to strengthen VC. Two recent electron-microscopy studies of V_6C_5 have revealed two of the strengthening mechanisms.

Hannink and Murray [15] have investigated the influence of domain boundaries on the room-temperature hardness of V_6C_5. Hannink measured a 13% decrease in hardness when the axial-domain size was increased, by adjusting the rate of cooling through the order-disorder transition, from 0.3 to 7.5 μm. Two possible models for domain-boundary hardening were suggested, one involving a dislocation-domain boundary interaction similar to the Hall-Petch [44, 45] analysis for grain-boundary hardening and a second based on Cottrell's [46] model for anti-phase domain-boundary hardening. In a second paper, Hannink *et al* [47] have demonstrated that dislocations in V_6C_5 leave APB trails. These trails will also act to increase the strength of V_6C_5 with respect to the disordered carbides. Removal of these obstacles to dislocation motion should result in a marked change in hardness.

Acknowledgements

The author wishes to thank Dr D. Tabor, FRS, for his interest and encouragement; Dr R. H. J. Hannink and Dr M. J. Murray for their very valuable comments and criticisms during the experimental, analytical, and writing portions of this research; Dr W. S. Williams for discussions of the results and manuscript; and Dr N. Gane for discussions of the analysis of hardness data. The Science Research Council is gratefully acknowledged for the research grant which supported this work.

References

1. E. K. STORMS, "The Refractory Carbides" (Academic Press, New York, 1967) p. 229.
2. J. VENABLES, P. KAHN, and R. LYE, *Phil. Mag.* **18** (1968) 177.
3. W. S. WILLIAMS, *J. Appl. Phys.* **35** (1964) 1329.

4. R. HILL, "The Mathematical Theory of Plasticity" (Clarendon Press, Oxford, 1950).
5. D. TABOR, "The Hardness of Metals" (Clarendon Press, Oxford, 1951).
6. *Idem, Rev. Phys. Tech.* **1** (1970) 145.
7. J. H. WESTBROOK, *Acta Metallurgica* **3** (1955) 104.
8. A. MIYOSHI and A. HARA, *J. Jap. Soc. Powder and Powder Met.* **12** (1965) 78.
9. A. ATKINS and D. TABOR, *Proc. Roy. Soc.* **A292** (1966) 441.
10. R. D. KOESTER and D. P. MOAK, *J. Amer. Ceram. Soc.* **50** (1967) 290.
11. J. H. WESTBROOK and E. R. STOVER, in "High Temperature Materials and Technology", ed. I. E. Campbell and E. M. Sherwood (Wiley, New York, 1967) p. 312.
12. G. V. SAMSONOV, M. S. KOVALCHENKO, V. V. DZEMELINSKII, and G. S. UPADYAYA, *Phys. Stat. Sol. (a)* **1** (1970) 327.
13. G. E. HOLLOX, *Mater. Sci. Eng.* **3** (1968/69) 121.
14. A. KELLY and D. J. ROWCLIFFE, *J. Amer. Ceram. Soc.* **50** (1967) 253.
15. R. H. J. HANNINK and M. J. MURRAY, *Acta Metallurgica* **20** (1972) 123.
16. M. E. PACKER and M. J. MURRAY, *J. Phys. E: Sci. Instrum.* **5** (1972) 246.
17. W. S. WILLIAMS and R. D. SCHAAL, *J. Appl. Phys.* **33** (1962) 955.
18. W. S. WILLIAMS, in "Propriétés Thermodynamiques Physique et Structurales des Dérivés Semi-Métallique" (Editions du Centre National de la Recherche Scientifique, Paris, 1967) pp. 181-189.
19. D. J. ROWCLIFFE, private communication, 1971.
20. D. L. KOHLSTEDT and R. H. J. HANNINK, in preparation.
21. R. H. J. HANNINK, D. L. KOHLSTEDT, and M. J. MURRAY, *Proc. Roy. Soc.* **A326** (1972) 409.
22. D. J. ROWCLIFFE and W. J. WARREN, *J. Mater. Sci.* **5** (1970) 345.
23. C. A. BROOKES, J. B. O'NEILL, and B. A. W. REDFERN, *Proc. Roy. Soc.* **A332** (1971) 73.
24. J. B. CONKLIN and D. J. SILVERSMITH, *Int. J. Quantum Chem.* **IIS** (1968) 243.
25. J. PIPER, *J. Appl. Phys.* **33** (1962) 2394.
26. O. A. GOLIKOVA, F. L. FEIGEL'MAN, A. I. AVGUSTINIK, and G. M. KLIMASKIN, *Fiz. Tekhn. Polup.* **1** (1967) 293.
[English trans.: *Sov. Phys. Semicond.* **1** (1967) 236.]
27. D. M. MARSH, *Proc. Roy. Soc.* **A279** (1964) 420.
28. K. L. JOHNSON, *J. Mech. Phys. Solids* **18** (1970) 115.
29. D. A. SPECK and B. R. MICCIOLI, "Advanced Ceramic Systems for Rocket Nozzle Applications", Carborundum Company Rept., October, 1968.
30. J. H. WESTBROOK, *WADC Tech. Rept.* 58-304, Contract AF 33 (616)-5511, August, 1958.
31 M. J. MURRAY, private communication, 1972.
32. F. KEIHN and R. KEBLER, *J. Less-Common Metals* **6** (1964) 484.
33. M. H. LEIPOLD and T. H. NIELSEN, *J. Amer. Ceram. Soc.* **47** (1964) 419.
34. D. W. LEE and J. S. HAGGERTY, *ibid* **52** (1969) 641.
35. G. E. HOLLOX and R. E. SMALLMAN, *Proc. Brit. Ceram. Soc.* **1** (1964) 211; *J. Appl. Phys.* **37** (1966) 818.
36. P. G. SHEWMON, "Diffusion in Solids" (McGraw-Hill, New York, 1963) p. 178.
37. J. WEERTMAN, *J. Appl. Phys.* **26** (1955) 1213.
38. A. G. ATKINS, A. A. SILVERIO, and D. TABOR, *J. Inst. Metals* **94** (1966) 369.
39. S. SARIAN, *J. Appl. Phys.* **40** (1969) 3515.
40. S. SARIAN and J. C. CRISCIONE, *ibid* **38** (1967) 1794; S. SARIAN, *ibid* **39** (1968) 5036; *ibid* **39** (1968) 3305.
41. D. L. KOHLSTEDT, W. S. WILLIAMS, and J. B. WOODHOUSE, *ibid* **41** (1970) 4476.
42. W. S. WILLIAMS, in "Progress in Solid State Chemistry", eds. H. Reiss and J. O. McCaldin, 1971 (Macmillan, New York, Vol. VI).
43. L. E. TOTH, "Transition Metal Carbides and Nitrides" (Academic Press, New York, 1971).
44. E. O. HALL, *Proc. Roy. Soc.* **1364** (1951) 747.
45. N. J. PETCH, *J. Iron Steel Inst.* **174** (1953) 25.
46. A. H. COTTRELL, "Relation of Properties to Microstructure" (ASM, Metals Park, 1954) p. 131.
47. R. H. J. HANNINK, M. J. MURRAY, and M. E. PACKER, *Phil. Mag.* in press.

Received 12 June and accepted 22 December 1972.